Demodulation of acoustic telemetry binary phase shift keying signal based on high-order Duffing system*

Bing-Nan Yan(燕并男)[1,2,†], Chong-Xin Liu(刘崇新)[1], Jun-Kang Ni(倪骏康)[1], and Liang Zhao(赵亮)[3]

[1] School of Electrical Engineering, Xi'an Jiaotong University, Xi'an 710049, China
[2] College of Electrical Engineering, School of Xi'an Shiyou University, Xi'an 710065, China
[3] Xi'an Thermal Power Research Institute Co. Ltd, Block A, Boyuan Science & Technology Building, Xi'an 710054, China

(Received 11 April 2016; revised manuscript received 16 June 2016; published online 25 August 2016)

In order to grasp the downhole situation immediately, logging while drilling (LWD) technology is adopted. One of the LWD technologies, called acoustic telemetry, can be successfully applied to modern drilling. It is critical for acoustic telemetry technology that the signal is successfully transmitted to the ground. In this paper, binary phase shift keying (BPSK) is used to modulate carrier waves for the transmission and a new BPSK demodulation scheme based on Duffing chaos is investigated. Firstly, a high-order system is given in order to enhance the signal detection capability and it is realized through building a virtual circuit using an electronic workbench (EWB). Secondly, a new BPSK demodulation scheme is proposed based on the intermittent chaos phenomena of the new Duffing system. Finally, a system variable crossing zero-point equidistance method is proposed to obtain the phase difference between the system and the BPSK signal. Then it is determined that the digital signal transmitted from the bottom of the well is '0' or '1'. The simulation results show that the demodulation method is feasible.

Keywords: acoustic telemetry, BPSK demodulation, Duffing system

PACS: 05.45.–a, 05.40.–a **DOI:** 10.1088/1674-1056/25/10/100502

1. Introduction

In order to grasp the downhole situation immediately, logging while drilling (LWD) technology is adopted. An oil drilling technology is used to obtain the physical parameters of the rock formation or drilling parameters measured while drilling and propagating data to the ground.[1] So far, the main wireless transmission technologies are mud pulse, electromagnetic (EM) telemetry and acoustic telemetry. Unfortunately, the throughput of the mud pulse system is too low to satisfy the volume of data and its magnitude is only about a few bits per second. An EM system will fail if the formation resistivity is low or the resistivity profile is too complex. The attenuation of wave is severe and the transmission distance is short.[2] Both methods can rarely be applied successfully to modern drilling; the third method, called acoustic telemetry, can potentially overcome the shortcomings of them.

In the acoustic telemetry system, the downhole information sensed by the sensor is converted into electrical signals, which are carried by acoustic stress waves. The waves propagate along the drill strings until the signals are picked up by a surface receiver. This transmission does not depend on the drilling fluid, and is not affected by the properties of the formation. Its advantages, such as simple device framework, low cost, and high data rate, means it has broad application prospects in underbalanced drilling conditions. Therefore, the acoustic telemetry technology has become a hot research point in oil field drilling telemetry. If the technology is successfully used in LWD, there are two problems that need to be solved. One is how to choose the carrier frequency. Previous studies[3–6] investigated the transmission of acoustic waves along the drill pipes and drew the conclusion that the channel formed by the drill string has a comb filter structure with the passband and stopband showing up in turn. The other is how to select an efficient signal modulation/demodulation method and a signal detection technology.[7–10] How the signal is successfully transmitted to the ground is critical for acoustic telemetry technology.

Binary phase shift keying (BPSK) is a digital two-phase modulation scheme which modulates carrier waves based on a binary baseband signal in acoustic telemetry. It possesses high anti-noise performance and bandwidth utilization efficiency. In Ref. [7] the acoustic telemetry tool schematic was studied by the XACT Institute. The voltage across the piexoelectric tranducer (PZT) stack was modulated to generate an acoustic carrier wave with data encoded via BPSK. Through field testing it was proved that real-time annular pressure data were consistently transmitted to the surface utilizing acoustic telemetry. A BPSK signal was successfully transmitted at a

*Project supported by the National Natural Science Foundation of China (Grant No. 51177117) and the National Key Science & Technology Special Projects, China (Grant No. 2011ZX05021-005).

†Corresponding author. E-mail: bnyan@xsyu.edu.cn

© 2016 Chinese Physical Society and IOP Publishing Ltd

depth of 3083 ft (1 ft = 3.048×10^{-1} m), with carrier frequencies being 830 Hz, 1030 Hz, and 1230 Hz.[8] A bit rate of 30 bps could be achievable.

In the present paper, a new BPSK demodulation scheme based on Duffing chaos is investigated. Chaos is a form of nonlinear movement[11,12] and the Duffing system describes the motion of the system of nonlinear elasticity, in which the driving force is sinusoidal. Therefore, it can be widely used in signal detection.[13–20] In Ref. [13], a quantitative detection method for weak sinusoidal signals based on the sensitivity of chaotic parameters in a particular state was proposed. The simulation experiments showed that the immunity to noise was enhanced with the increase of amplitude detected with guaranteed precision. Authors in Ref. [15] studied the weak sinusoidal signal detection under strong ocean background noise based on the intermittent chaos Duffing oscillator using Hilbert transform. The results proved that SNR was increased by 4.4 dB compared with those obtained by using the basic methods. Authors in Ref. [16] studied the stochastic resonance characteristic of a two-dimensional (2D) Duffing oscillator under the adiabatic assumption. In large parameter conditions, it revealed the mechanism of signal detection by Duffing oscillator stochastic resonance. In Ref. [17] a new method of detecting weak pulse signals based on an extended-Duffing oscillator was proposed. The approach could effectively expand the frequency detection range for weak signal detection. Authors in Ref. [19] developed a stochastic averaging procedure for the Duffing–Rayleigh system by using the generalized harmonic functions. The results showed that the fractional order, the coefficient of the fractional derivative, the noise intensity, and the natural frequency played important roles in the response of the system.

Only the Holmes Duffing equation was extensively studied in the above references. In Ref. [21], the simulation showed when the order of the Duffing equation was increased, the sensitivity of the signal detection was enhanced and the working stability was better. Therefore, the equation is advanced, a high-order system is given in order to enhance the signal detection capability and it is realized through building a virtual circuit by using EWB in this paper. A new BPSK demodulation scheme is proposed based on the intermittent chaos phenomena of the high-order Duffing system. The approach helps to detect the BPSK signal transmitted from the bottom successfully.

The rest of the paper is organized as follows. In Section 2, the high-order Duffing system is described and the main parameters are given according to the simulation results. In Section 3, the detection principle of an acoustic telemetry signal based on the high-order Duffing system is studied. The results are analyzed in Section 4 and the conclusions are drawn in the last section.

2. Modeling and simulation of high-order Duffing system

The Holmes Duffing equation is described as follows:

$$\ddot{x}(t) + r\dot{x}(t) - x(t) + x^3(t) = A\cos(t), \tag{1}$$

where $x(t)$ is the state variable; r is the damping ratio; $A\cos(t)$ is named the periodic driving force, in which A is the amplitude; $-x(t) + x^3(t)$ is defined as the nonlinear restoring force. In order to improve the detection sensitivity and enhance working stability, the order of the nonlinear restoring force is increased by two. Equation (1) is rewritten as

$$\ddot{x}(t) + r\dot{x}(t) - x^3(t) + x^5(t) = A\cos(t). \tag{2}$$

The nonlinear restoring function is in the highorder form. The global nature of the system is more complex. It is needed to analyze the dynamic behavior.

2.1. Dynamic behavior analysis of the high-order Duffing system

Equation (2) is rewritten in the form of a state space equation:

$$\begin{cases} \dfrac{\mathrm{d}x}{\mathrm{d}t} = y, \\ \dfrac{\mathrm{d}y}{\mathrm{d}t} = -ry + x^3 - x^5 + A\cos(t). \end{cases} \tag{3}$$

Since r is a constant, the state of the system changes with parameter A. When $A \neq 0$, the system presents complex dynamic states and goes through a periodic oscillation state, homoclinic-orbit state, bifurcation state, and lastly into the chaotic state. When A is equal to A_{d} (the bifurcation threshold), the state of the system changes from a critical chaotic state to a large periodic state. Further if the value of A is increased to a value that is slightly larger than the bifurcation threshold, the system reaches a large periodic state. In this paper, the damping ratio r is given as 0.5. The system angular frequency is 1 rad/s and the initial values are $[x(0), x'(0)] = [0, 0]$. The simulation step is set to be 0.01. The simulation is carried out. The system bifurcation diagram is shown in Fig. 1, and the simulation results of the critical chaotic state and the large periodic state are shown in Fig. 2. According to these results, the bifurcation threshold is determined to be $A_{\mathrm{d}} = 0.7369$.

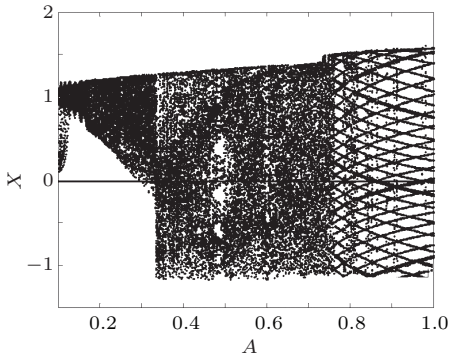


Fig. 1. Bifurcation diagram of the system under consideration.

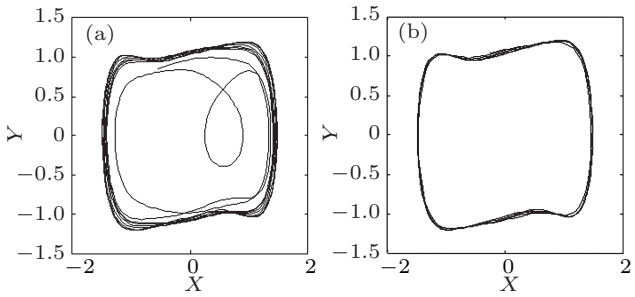


Fig. 2. Large periodic state when $A_d = 0.7369$: (a) the critical chaotic state, and (b) the large periodic state.

The simulation results show that extremely small changes of A can cause fundamental changes of the system state. When the system is driven to the critical chaotic state, if the value of A fluctuates around the threshold, the Duffing system would be driven to a chaotic state or large periodic state. It is intermittent chaos, which is the principle of signal detection based on the Duffing system.

Specifically, firstly, adjust the amplitude of the driving force to make the Duffing system go into the critical chaotic state. Secondly, add the BPSK signal as the perturbation of the driving force to the left of the Duffing equation. Finally, observe the change of the system state and thereby demodulate the BPSK signal based on the sensitivity of the Duffing oscillator to the perturbation.

2.2. Virtual circuit implementation of the high-order Duffing system

To enhance the sensitivity of signal detection, the Duffing equation is improved. The intermittent chaos phenomenon is simulated to obtain critical parameters. The Duffing system is realized through building a virtual circuit by using EWB. The schematic circuit diagram is shown in Fig. 3, in which ideal operational amplifiers, multipliers, resistances and capacitors are used. The value of the amplitude of the periodic driving force is set to be 18 V, and the frequency is set to be 1 Hz. By adjusting the circuit parameters, the possibility to implement such a physical system is investigated. The simulation results are shown in Fig. 4, and the system is at the chaotic state according to the X–Y diagram.

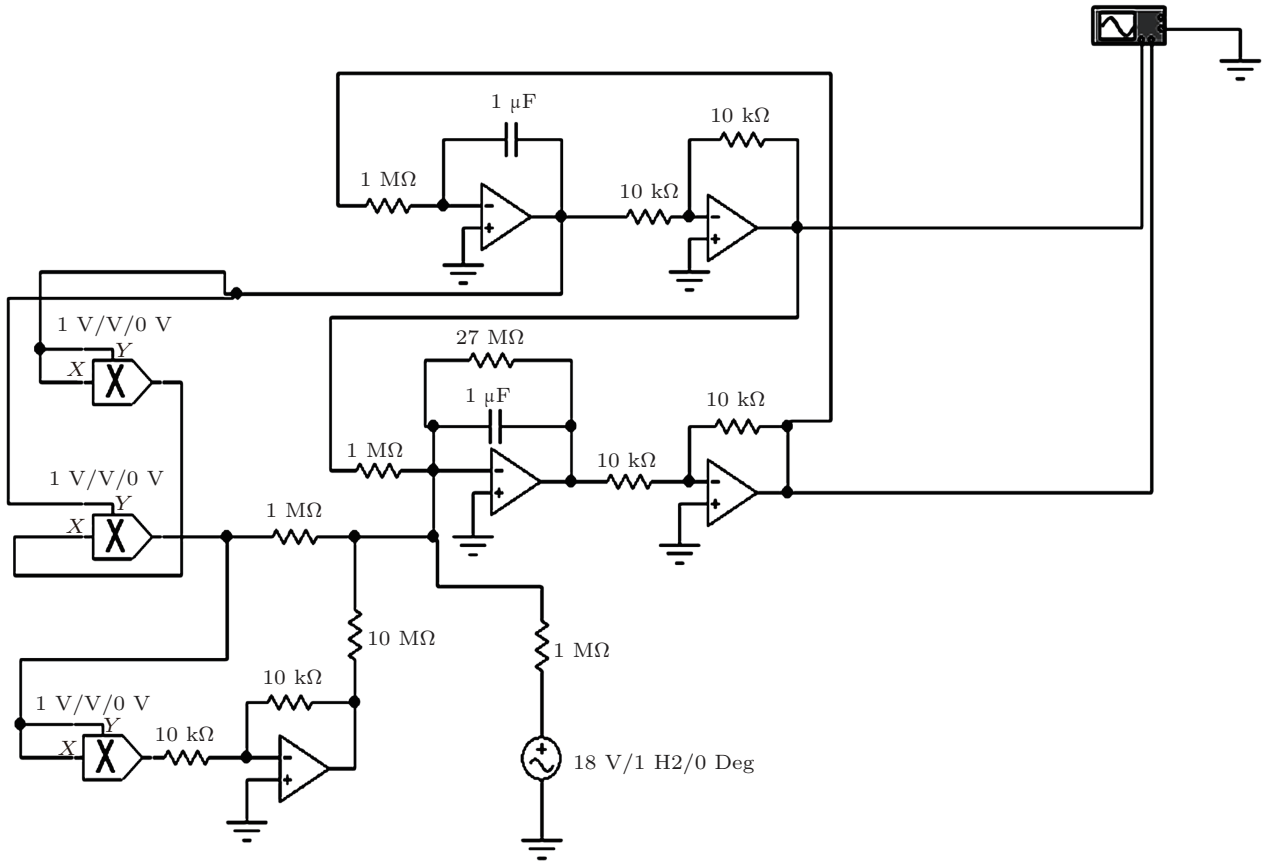


Fig. 3. Schematic circuit diagram of the high-order Duffing system.

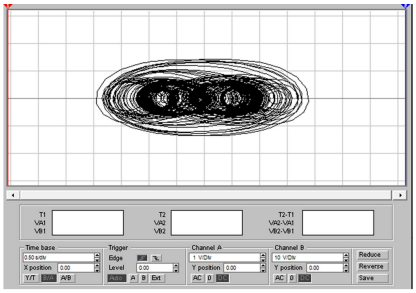


Fig. 4. Simulation results of X–Y diagram.

3. Detection principle of acoustic telemetry signal based on high-order Duffing system

3.1. BPSK modulation mechanism

The BPSK signal is expressed as

$$S_x(t) = a_x \cos(w_c t + \varphi_x), \quad x = 1,2, \tag{4}$$

where a_x is the signal amplitude; w_c is the signal angle frequency; φ_x is the signal initial phase which has two values: $\varphi_1 = 0$ and $\varphi_2 = \pi$. When digital signal '0' is sent from the bottom of the well, $\varphi_1 = 0$ and the BPSK is modulated as

$$s_1(t) = a_1 \cos(\omega_c(1+\Delta\omega)t).$$

When digital signal '1' is sent from the bottom of the well, $\varphi_2 = \pi$, and the BPSK is modulated as $s_2(t) = a_2 \cos(\omega_c(1+\Delta\omega)t + \pi)$.

3.2. Analyses of intermittent chaos phenomena and parameters settings

Downhole acoustic signals are transmitted along the drill pipe to the ground. In 1989, Drumheller analyzed the frequency characteristics of longitudinal waves transmitting along the ideal drill pipes. He noted that the acoustic transmission channel was the comb filter structure with alternating the passband and stopband. Therefore, only by selecting the frequency within the passband, could the acoustic signal successfully transmit to the ground and be received by the receiver. It is assumed that the downhole signal is modulated as Eq. (4), in which angle frequency is set as ω_c. Then the periodic driving force parameters of the system are set, such as the amplitude given as A_0, the phase as φ, and the angle frequency as ω. The angle frequency value is around ω_c, which satisfies $\omega_c = \omega(1+\Delta\omega)$ ($\Delta\omega$ is the frequency difference between the two angle frequencies). Let $t = \omega\tau$, and equation (2) is rewritten as

$$\frac{1}{\omega^2}\ddot{x}(\tau) + \frac{r}{\omega}\dot{x}(\tau) - x^3(\tau) + x^5(\tau) = A_0 \cos(\omega\tau + \varphi). \tag{5}$$

Substituting Eq. (4) into Eq. (5) one can obtain

$$\frac{1}{\omega^2}\ddot{x}(\tau) + \frac{r}{\omega}\dot{x}(\tau) - x^3(\tau) + x^5(\tau)$$
$$= A_0 \cos(\omega\tau + \varphi) + a_x \cos[\omega(1+\Delta\omega)\tau + \varphi_x], \quad x = 1,2. \tag{6}$$

Multiply both sides of the above equation by ω^2, the resulting equation can be simplified into the following equation:

$$\ddot{x}(\tau) + r\omega\dot{x}(\tau) - \omega^2[x^3(\tau) - x^5(\tau)]$$
$$= \omega^2 A(\tau)\cos(\omega\tau + \theta(\tau)), \tag{7}$$

where

$$A(\tau) = \sqrt{A_0^2 + 2A_0 a_x \cos(\omega\Delta\omega t + \Delta\varphi) + a_x^2}, \tag{8}$$

$$\theta(\tau) = \varphi + \arctan\frac{a_x \sin(\omega\Delta\omega t + \Delta\varphi)}{A_0 + a_x\cos(\omega\Delta\omega t + \Delta\varphi)}. \tag{9}$$

In Eq. (7), $\omega^2 A(\tau)$ is the amplitude of the total driving force. It is the time-varying sinusoidal function. Its value varies periodically between $\omega^2(A_0 - a_x)$ and $\omega^2(A_0 + a_x)$, and the period is calculated as $T = 2\pi/\omega\Delta\omega$. $\theta(\tau)$ is the initial phase of the total driving force. The simulation result shows that $\theta(\tau)$ is also a time-varying sinusoidal function, and in Ref. [22] it was pointed out that $\theta(\tau)$ is a function of $A(\tau)\Delta\varphi$ which is the phase difference between the system driving force and the BPSK signal. It is calculated from

$$\Delta\varphi = \varphi_x - \varphi. \tag{10}$$

In order to simplify the system, we define $\varphi = \varphi_1$. It means that when the signal '0' is transmitted from the bottom $\Delta\varphi = 0$.

The simulation study shows that if $A_0 < 0.7a_x$ or $A_0 > a_x$, the intermittent chaos phenomenon of the Duffing system is not obvious. Then, we set $A_0 = (0.7 \sim 1)a_x$ to enhance the accuracy of signal demodulation. Because of the serious attenuation of the signal transmitting from the bottom to the surface, a_x is very small. The received signal firstly needs to be amplified and a reasonable value of A_0 is set to meet the conditions mentioned above.

Set $A_0 = 0.736$, $a_x = 1$, $\omega = 1$ and observe the changes of the system state, then it will be found that $A_d \in (0.7368, 0.7369)$. When $A(\tau) > A_d$, the system state is a large periodic state; when $A(\tau) < A_d$ the system state is a chaotic state. This is why the intermittent chaos phenomenon occurs.

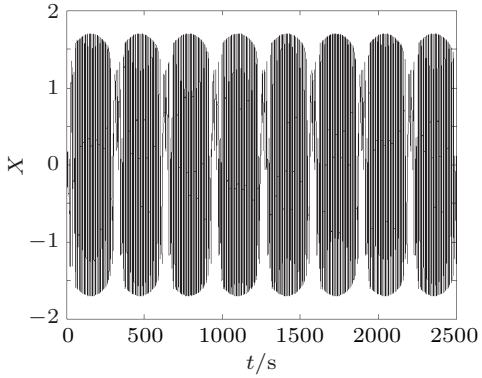


Fig. 5. Intermittent chaos phenomenon with $\Delta\omega = 0.02$.

When $\Delta\omega = 0.02$, the simulation results are shown in Fig. 5. When $\Delta\omega = 0.06$, the simulation results are shown in Fig. 6.

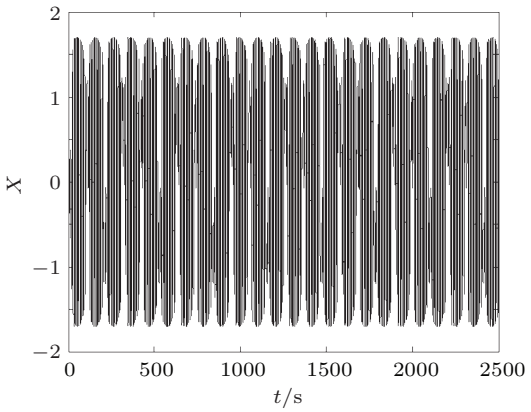


Fig. 6. Intermittent chaos phenomenon with $\Delta\omega = 0.06$.

From Figs. 5 and 6, it is shown that when $\Delta\omega$ is larger, the intermittent chaos phenomenon becomes inconspicuous or even disappears gradually. It is because it usually takes more than one cycle time to stabilize the response of the system state. If $\Delta\omega$ is too large, it leads to a very fast change of $A(\tau)$. Thus, the excitation does not last long enough in the process of the system phase change, and the system cannot respond very well when the change is so fast. The intermittent chaos phenomenon loses its regularity. In addition, when $\Delta\omega$ is too small, $A(\tau)$ varies insignificantly for a long period. It requires a long time for the system state to change, which means that the system can maintain the large periodic state or the chaotic state in a long stage. Therefore, based on the simulation study, $\Delta\omega$ is set to be between 0.02ω and 0.04ω to obtain the obvious intermittent chaos phenomenon. When $\Delta\omega = 0.02\omega$, the X–Y diagram is shown in Fig. 7.

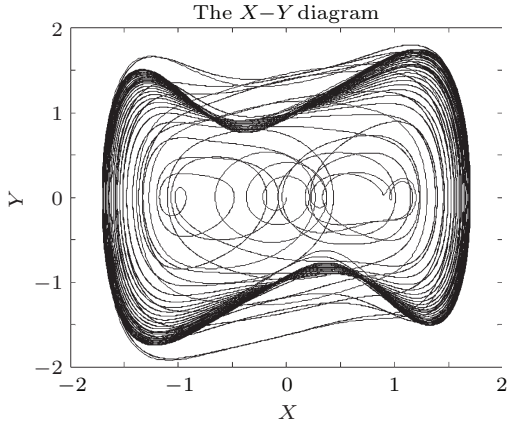


Fig. 7. The X–Y diagram.

3.3. BPSK signal demodulation scheme

From the above analysis, the bifurcation threshold value is set as $(A_0 - a_x, A_0 + a_x)$. It is supposed that when $\cos(\omega\Delta\omega t + \varphi_x) = c (c \in [0,1])$, $A(\tau) = A_d$. Then if $\cos(\omega\Delta\omega t + \phi) > c$, the state of the system is the large periodic state whose period is described by T_1 shown in Fig. 8. If $\cos(\omega\Delta\omega t + \phi) < c$, the state of the system is a chaotic state, whose period is described by T_2 shown in Fig. 8.

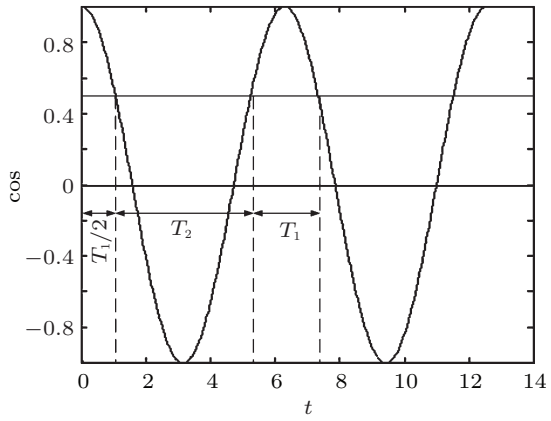


Fig. 8. Time intervals of the two system states.

When $\omega\Delta\omega t + \Delta\varphi = 0$, then $\cos(\omega\Delta\omega t + \Delta\varphi) = 1$ and the value of $A(\tau)$ is maximum. At this time, if $A(\tau) > A_d$, the system state is a large periodic state. As time increases, when $t = T_1/2$, $\cos(\omega\Delta\omega t + \Delta\varphi)$ decreases to c and $A(\tau)$ reduces from the maximum value to A_d. The system transfers from the large periodic state into the critical chaotic state. Because the cosine waveform has axial symmetry, the change of the system also needs the same time when $\cos(\omega\Delta\omega t + \varphi)$ increases from c to 1.

It can be concluded that when $t_z = (2k\pi - \Delta\varphi)/\omega\Delta\omega$, $\cos(\omega\Delta\omega t + \Delta\varphi) = 1$ and the system is at the midpoint of the large periodic state. The time is set as t_1 when the system goes into the large periodic state from the chaotic state. The time is set as t_2 when the system goes into the chaotic state from the large periodic state. If both of the times are found, the midpoint of the state is calculated as

$$t_z = \frac{t_1 + t_2}{2} = \frac{2k\pi - \Delta\varphi}{\omega\Delta\omega},$$

and the phase difference is

$$\Delta\varphi = 2k\pi - \omega\Delta\omega\left(\frac{t_1 + t_2}{2}\right). \tag{11}$$

It is the method to calculate $\Delta\varphi$.

Since the initial phase of the system is equal to the phase of signal '0', if $\Delta\varphi = 0$, it can be determined that the digital signal transmitting from the bottom of the well is '0'. If $\Delta\varphi = \pi$, the digital signal is '1'.

In this paper, a system variables crossing zero-point equidistance method is used to calculate t_1 and t_2. When the system is at the large periodic state, the distances of variables crossing the zero-point are the same. Unfortunately when the system is at the chaotic state, there is no such feature. The

method is adopted to record the equidistance ten times to ensure the reliability of the algorithm. If the distance is the same every time, it can be determined that the system enters into the large periodic state. Otherwise, the system is at the chaotic state. Through this process t_1 and t_2 are recorded to calculate $\Delta\varphi$.

4. Simulation and result analysis

Assume that the BPSK signal '0/1' is sent from the bottom of the well, and set the system parameters as the above to make the system meet the intermittent chaos conditions.

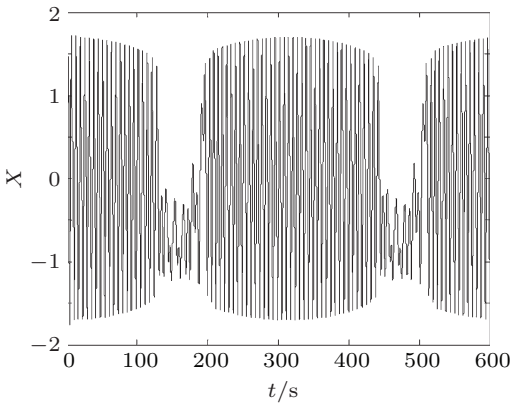


Fig. 9. Timing simulation diagram while transmitting '0' when $t \in (0,600)$.

When the signal sent is '0', the intermittent chaos phenomenon is shown in Fig. 9 with $t \in (0,600)$. In order to demonstrate the system is chaotic in a certain time series, the dynamic behavior of the Lyapunov exponent is simulated. The result is shown in Fig. 10. When $A > A_d$, the system is converted from the chaotic state into the large periodic state; when $A < A_d$, the system is transformed from the large periodic state into the chaotic state. The dynamic behavior is consistent with the principles discussed above.

When $t = 200$ nearly, the system is converted from the chaotic state into the large periodic state. When $t = 430$ nearly, the system is transformed from the large periodic state into the chaotic state. The variables crossing the zero-point in the interval $t \in (180,450)$ are recorded. The results are shown in Tables 1 and 2. It is found that the critical time point is $t_{11} = 189.08$ when the system is transformed from the large periodic state into the chaotic state and the time point is $t_{12} = 443.72$ when the system is converted from the chaotic state into the large periodic state. Using this method the amount of computation to find the critical time point is reduced. Substituting t_{11} and t_{12} into Eq. (11), with $k = 1$ and $\Delta\varphi = -0.05 \approx 0$, the signal sent is determined to be '0'.

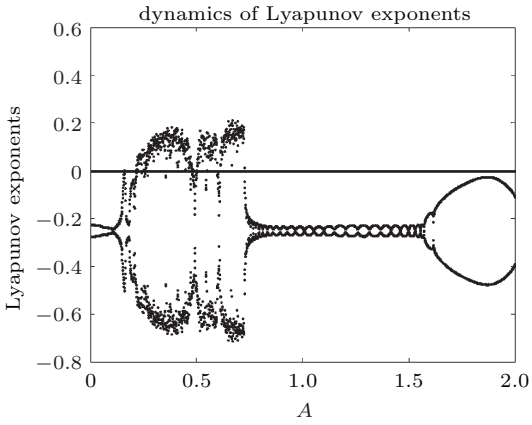


Fig. 10. Dynamic behavior of the Lyapunov exponent while transmitting '0'.

Table 1. Variables crossing zero-point statistics when the system is transformed from the chaotic state into the large periodic state while transmitting '0'.

t	177.72	179.68	189.54	198.08	201.36	204.40	207.30	210.16	213.11	216.20
$X(t)$	–0.001	–0.003	0.003	0.003	–0.003	–0.006	–0.001	0.001	0.001	0.003

Table 2. Variables crossing zero-point statistics when the system is converted from the large periodic state into the chaotic state while transmitting '0'.

t	420.50	423.71	426.92	430.16	433.42	436.73	440.12	443.72	491.89	493.83
$X(t)$	–0.004	–0.004	–0.002	–0.004	0.002	–0.004	0.002	0.003	0.000	0.000

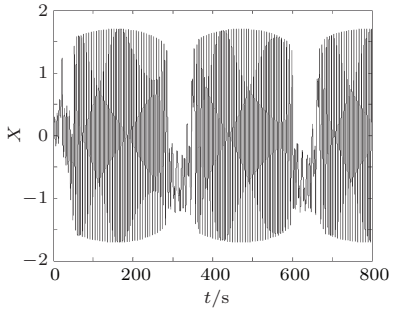


Fig. 11. Timing simulation diagram while transmitting '1'.

Similarly, when the signal sent is '1', the intermittent chaos phenomenon is shown in Fig. 11 with the interval $t \in (0,600)$.

The variables crossing the zero-point in the interval $t \in (350,650)$ are recorded. The results are shown in the following Tables 3 and 4. The critical time points are $t_{21} = 355.16$ and $t_{22} = 600.80$. By substituting t_{21} and t_{22} into Eq. (11), with $k = 2$ and $\Delta\varphi = 3.00 \approx \pi$, the signal sent is determined to be '1'.

Table 3. Variables crossing zero-point statistics when the system transformed from the chaotic state into the large periodic state while transmitting '1'.

t	336.75	346.61	355.16	358.44	361.47	364.38	367.24	370.19	373.28	376.41
$X(t)$	0.001	–0.004	0.003	–0.003	0.005	0.000	0.000	0.002	0.003	–0.003

Table 4. Variables crossing zero-point statistics when the system is converted from the large periodic state into the chaotic state while transmitting '1'.

t	584.00	587.24	590.50	593.80	597.20	600.80	648.96	650.91	660.77	669.32
$X(t)$	–0.001	–0.004	0.002	0.005	0.002	0.003	0.000	0.000	–0.003	0.002

The accuracy of the simulation is affected by the simulation step. The step cannot be exactly chosen so that the time for the variable to cross the zero point is picked up each time. In this paper, the time when the variable crosses the zero-point is determined by the absolute value of the variable. If the variable changes from a negative value to a positive value, the crossing zero-point is where its absolute value is closest to zero. Therefore, when variables of the crossing zero-point equidistance method are used to judge the two states of the system, there are errors and $\Delta\varphi$ calculated is an approximate value. But the phases of the BPSK signal are just 0 and π, so the error can be limited in a permissible range. To reduce the error, a smaller simulation step should be used. As a result, the calculating increases accordingly.

5. Conclusions

In the present work, the dynamic behavior of a high-order Duffing system is studied. The virtual circuit is built, and the intermittent chaos phenomenon is investigated. Based on the above, a new demodulation method of an acoustic telemetry BPSK signal is proposed. The system variables crossing zero-point equidistance method is adopted to find t_1 and t_2 and the phase difference can be obtained from Eq. (11). Finally, the digital signal transmitted from the bottom of the well is determined to be '0' or '1'. The simulation results show that the demodulation method is feasible. There is a lot of noise produced in the underground operation, but the Duffing system is immune to noise. Therefore, further studies are needed to find how to detect the BPSK signal from the noise using this method and to achieve the real applications of the downhole data detection.

Acknowledgment

We thank our group and other colleagues for their scientific contributions to this work.

References

[1] Zhang X Y, Wang J N and Guo Y J 2006 *Well Logging Technology* **30** 11 (in Chinese)
[2] Zhu K B, Nie Z P and Sun X Y 2013 *Acta Phys. Sin.* **62** 060202 (in Chinese)
[3] Drumheller D S 1989 *J. Acoust. Soc. Am.* **85** 1048
[4] Neff J M and Camwell P L 2007 *SPE* 105021
[5] Vimal Shah, Wallace Gardner 2004 *SPE* 88636
[6] Zhao G S, Guan Z C, Du Z C, Huang M Q and Wang W 2013 *Acta Petrolei Sinica* **34** 152 (in Chinese)
[7] Reeves M E, Camwell P L and McRory J 2011 *SPE* 145566
[8] Gao L, Finley D,Gardner W Robbins C, Linyaev E, Moore J, Memarzadeh M and Johnson D 2006 *SPE* 98948
[9] Kevin D Fink and Pirooz Najafi (U.S. Patent) 0177596 [2010-07-15]
[10] Zhang H, Li A Z and Qu J H 2007 *Well Logging Technology* **31** 285 (in Chinese)
[11] Xie Q, Hu B, Chen K F, Liu W H and Tan X 2015 *Chin. Phys. B* **24** 110505
[12] Zhang Z Y, Feng X Q, Yao Z H and Jia H Y 2015 *Chin. Phys. B* **24** 110503
[13] Li Y, Yang B J and Shi Y W 2003 *Acta Phys. Sin.* **52** 52605 (in Chinese)
[14] Li Y, Xu K, Yang B J, Yuan Y and Wu N 2008 *Acta Phys. Sin.* **57** 3353 (in Chinese)
[15] Chen Z G, Li Y A and Chen X 2015 *Acta Phys. Sin.* **64** 200502 (in Chinese)
[16] Leng Y G, Lai Z H, Fan S B and Gao Y J 2012 *Acta Phys. Sin.* **61** 230502 (in Chinese)
[17] Zeng J Z, Zhou Y and Hu K 2015 *Acta Phys. Sin.* **64** 070505 (in Chinese)
[18] Li C, Xu W, Wang L and Li D X 2013 *Chin. Phys. B* **22** 110205
[19] Zhang R R Xu W, Yang G D and Han Q 2015 *Chin. Phys. B* **24** 020204
[20] Wang Y C, Zhao Q C and Wang A B 2008 *Chin. Phys. B* **17** 2373
[21] Li Y and Yang B J 2007 *Chaotic Oscillator System* (L-Y) *and Detection* (Beijing: Science Press) pp. 25–33
[22] Zhai D Q, Liu C X, Liu R and Xu Z 2010 *Acta Phys. Sin.* **59** 816 (in Chinese)